

# Ribosome display and selection of single-chain variable fragments effectively inhibit growth and progression of microspheres in vitro and in vivo

Shangke Huang<sup>1</sup>  | Lu Feng<sup>1</sup> | Gaili An<sup>2</sup> | Xiaojin Zhang<sup>3</sup> | Zixuan Zhao<sup>4</sup> | Rui Han<sup>1</sup> | Fuxi Lei<sup>1</sup> | Yujiao Zhang<sup>1</sup> | Anqi Luo<sup>1</sup> | Xin Jing<sup>1</sup> | Lin Zhao<sup>1</sup> | Shanzhi Gu<sup>5</sup> | Xinhan Zhao<sup>1</sup> | Lingxiao Zhang<sup>1</sup>

<sup>1</sup>Department of Medical Oncology, the First Affiliated Hospital of Xi'an Jiaotong University, Xi'an, China

<sup>2</sup>Department of Clinical Oncology, Shaanxi Provincial People's Hospital, Xi'an, China

<sup>3</sup>Department of The Medical School of Shaoxing University, Shaoxing, China

<sup>4</sup>Elite Property Management Ltd., Saskatoon, SK, Canada

<sup>5</sup>College of Forensic Medicine, Xi'an Jiaotong University Health Science Center, Xi'an, China

## Correspondence

Shanzhi Gu, Department of College of Forensic Medicine, Xi'an Jiaotong University Health Science Center, Xi'an, China.

Email: gushanzhi@mail.xjtu.edu.cn

and

Xinhan Zhao and Lingxiao Zhang, Department of Medical Oncology, the First Affiliated Hospital of Xi'an Jiaotong University, Xi'an, China.

Emails: zhaoxinhanprof@163.com (X. Zhao); zhanglx86@sina.com (L. Zhang)

## Funding information

The National Natural Science Foundation of China, (Grant/Award Number: "No. 81272898")

Distinguishing the surface markers of cancer stem cells (CSCs) is a useful method for early diagnosis and treatment of tumors, as CSCs may participate in tumorigenesis and metastasis by migrating into the circulatory system. However, the potential targets of CSCs are expressed at low levels in the natural state and are always changing. Thus, dynamic screening has been reported to be an effective measure for exploring CSC markers. In recent years, diverse single-chain variable fragments (scFvs) have been widely used in immunotherapy. In this study, we determined that the scFvs, screened using RD, had a high affinity to microspheres and could inhibit their progression. We also observed that the selected scFvs underwent evolution in vitro, and antitumor-associated proteins were successfully expressed. Combined with chemotherapy, the scFvs had a synergistic effect on the inhibition of the microspheres' progression in vitro and in vivo, which could be ascribed to their high affinity for stem-like cells and the inhibition of the microspheres' collective behaviors. In addition, proteins inhibiting CD44<sup>+</sup>/CD24<sup>+</sup> and MAPK were involved. Our data indicated that dynamic screening of the scFvs in a natural state was of great significance in the inhibition of the microspheres in vitro and in vivo.

## KEYWORDS

CD44<sup>+</sup>/CD24<sup>+</sup>, microsphere, ribosome display, scFv, screening

**Abbreviations:** CSC, cancer stem cell; PRM, peptide-ribosome-mRNA; RD, ribosome display; scFv, single-chain variable fragment; VH, heavy chain genes; VL,  $\kappa$  or  $\lambda$  light chain genes.

Huang and Feng contributed equally to this work.

This is an open access article under the terms of the Creative Commons Attribution-NonCommercial License, which permits use, distribution and reproduction in any medium, provided the original work is properly cited and is not used for commercial purposes.

© 2018 The Authors. *Cancer Science* published by John Wiley & Sons Australia, Ltd on behalf of Japanese Cancer Association.

## 1 | INTRODUCTION

Cancer stem cells are considered to be cells with special characteristics in tumor metastasis.<sup>1</sup> In recent years, researchers have observed that the morphology and surface markers of CSCs could change with the environment,<sup>2,3</sup> and their behaviors were more collective than their parental cancer cells.<sup>4</sup> In addition, CSCs can result in cancer metastasis through circulatory system migration.<sup>5,6</sup> Targeted treatment in combination with chemotherapy has played an important active role in drug-resistant and metastatic cancer. However, the impact on CSCs still remains unclear.<sup>7</sup> Due to the small number of CSCs and the low expression of stem cell-associated markers in the natural state of solid tumors,<sup>8,9</sup> we have reasons to believe that a high-flux, sensitive, and efficient system for screening specific molecules of CSCs will be a significant method in the early diagnosis, prediction, and targeted therapy of CSCs. In this study, we used RD to screen scFvs, as they have a high affinity for antigens and are convenient for molecular modification *in vitro*.<sup>10</sup> Because of the diversity of scFv libraries, many antibodies and antigens have been selected and investigated in previous research.<sup>11,12</sup>

Antibody library display technology has been widely used by researchers of pharmacy and medical science.<sup>11</sup> The most important factor is to screen for antibodies with high affinity and specificity. In particular, RD is one of the most powerful *in vitro* display technologies used to screen for single chain antibodies.<sup>13</sup> During the translation process of RD, PRMs are formed. Following the PRM screening, the binding ligands of mRNA are enriched, and new mRNA can be amplified by RT-PCR. Next, new PRM can be formed and entered for the next round of screening. The sequence of the gene and the polypeptide can then be detected and separated. After repeating this several times, the molecules with a high specificity and affinity can be obtained.<sup>10,11</sup> As RDs can be modified or marked with incorporation of non-natural amino acids in protein synthesis, the technology is also an effective method to study protein evolution.<sup>14,15</sup>

The affinity recognition of multiple targets is an important treatment method for solid tumors based on our understanding of gene technology and CSC markers.<sup>16,17</sup> As we know, the CD44<sup>+</sup> CD24<sup>-/low</sup> lineage of breast cancer cells has been thought to be breast CSCs.<sup>18</sup> However, CD24<sup>+</sup> cells are considered more closely related to the early, highly invasive, and differentiated cells in mammary tumors.<sup>17,19</sup> We infer that CSCs themselves may always be in a dynamic balance and inhomogeneous collective state. As Reya et al<sup>20</sup> have suggested, cancer cells, stem cells, and CSCs may share a common signaling pathway. We suppose the best maker selection and treatment may be given consideration to the stemness and differentiation of CSCs. Based on several early research reports and our preliminary study analysis, we speculate that the CD44<sup>+</sup>/CD24<sup>+</sup> and MAPK pathways could play a shared role in proliferation and differentiation in cancer cells and CSCs.<sup>21-23</sup> In this study, a large-scale screening of clinically functional scFvs was explored. An RD was applied to screen for high-affinity and evolved scFvs with stem-like microspheres. Our data suggest that the screened scFvs alone or in combination with chemotherapy could effectively inhibit tumor proliferation and invasion *in vitro* and *in vivo*.

## 2 | MATERIALS AND METHODS

### 2.1 | Cell lines and culture

Details are provided in Document S1.

### 2.2 | Enrichment and sequencing of stem-like cells

Details are provided in Document S1.

### 2.3 | Cell surface markers analysis

Details are provided in Document S1.

### 2.4 | Xenograft tumor growth in athymic nude mice

Details are provided in Document S1.

### 2.5 | Establishment of solid phase cell membrane screening

Details are provided in Document S1.

### 2.6 | Patient specimens

Forty-five blood samples of breast cancer patients and 10 blood samples of breast adenoma or hyperplasia patients were acquired (Table S1). The rights of the patients were authorized by the Patient Care and Protection Committee of the First Affiliated Hospital of Xi'an Jiaotong University (Xi'an, China). All of the samples were collected from preoperative blood and within a 6-month period. For each fresh blood sample, at least 3 mL blood was centrifuged, and the lymphocytes were collected by Lymphocyte Separation Medium (Tianjin Steven Biological Products Technology, Tianjin, China) within 4 hours *in vitro*. Clinical analysis was based on preoperative blood routines.

### 2.7 | Construction of scFv library

Details are provided in Document S1.

### 2.8 | Molecular biology reagents and kits

Cell-free TNT T7 Quick for PCR DNA (L5540, rabbit reticulocyte lysate, and Transcend tRNA) and Transcend Non-Radioactive Translation Detection Systems (L5080 and streptavidin-HRP) were acquired from Promega (Madison, WI, USA). Taq DNA polymerase, gel elution kit QIAEX II, and the RNeasy clean-up kit were acquired from Qiagen (Shanghai, China). The Titan one-tube RT-PCR system was acquired from Roche (Basel, Switzerland). The primer sequences were obtained from the research of Marks et al<sup>24</sup> and followed the advances of other researchers<sup>12</sup> (Table S2). The 6× His tag, T7 joint,

ribosome binding sites and stem loop structure sequence library from bacteriophage M13 gene III were introduced (Table S3, Figure S1). Primers and the new scFvs were synthesized by Beijing Dingguo Biotechnology (Beijing, China) (Figure S2). The used scFvs were prepared in PBS containing 5 mmol/L MgCl<sub>2</sub> and were folded by denaturation at 85°C for 5 minutes followed by 10 minutes incubation at room temperature and refolding at 37°C for at least 15 minutes.<sup>25</sup>

## 2.9 | Real-time PCR analysis

Details are provided in Document S1 and Table S4.

## 2.10 | In vitro transcription and translation

Details are provided in Document S1.

## 2.11 | Affinity selection and RT-PCR

Details are provided in Document S1.

## 2.12 | Analysis of the translation proteins

Details are provided in Document S1.

## 2.13 | MTT assay

Details are provided in Document S1.

## 2.14 | Assessment of apoptosis

Details are provided in Document S1.

## 2.15 | Enzyme-linked immunosorbent assay

Details are provided in Document S1.

## 2.16 | Immunofluorescence assay

Details are provided in Document S1.

## 2.17 | Cell migration and invasion assays

Details are provided in Document S1.

## 2.18 | Immunohistochemical staining and evaluation

Details are provided in Document S1.

## 2.19 | Western blot analysis

Details are provided in Document S1.

## 2.20 | Statistical analysis

Details are provided in Document S1.

# 3 | RESULTS

## 3.1 | Anti-breast cancer scFvs and RD libraries were constructed

Total RNA was isolated from peripheral blood lymphocytes from blood samples of breast cancer patients (Figure 1A, Table S1). Single bands of the correct size of VH (approximately 340 bp) (Figure 1B, Table S2) and VL (V<sub>κ</sub> and V<sub>λ</sub>, approximately 325 bp) genes were obtained by PCR amplification using non-degenerative primers (Figure 1C,D). Next, the VH 3'- and VL 5'-ends were connected with the linker (Gly4Ser)<sub>3</sub> sequence by linker primers as the VH-linker and VL-linker (Figure 1E, F, Table S2). The diversity and abundance of the scFv library (size approximately 750 bp) was produced by the first overlap extension PCR through the VH-linker and VL-linker (Figure 1G,H). Approximately 18 μg purified PCR product was obtained and the scFv library contained a capacity of >10<sup>13</sup>. To increase the diversity of the library, we not only expanded all of the heavy and light chain variable regions but also screened the clinical samples on a larger scale. Clinical analysis indicated that the relatively stable construction of the scFv library had significantly higher numbers of peripheral lymphocytes ( $P = .0096$ ; Table S1), as well as a higher proportion of Leu/Lym ( $P = .0418$ ; Table S1). However, there was no significant association between Leu/Lym and tumor stage or receptor state in this population.

Next, the gene III fragment was amplified from the bacteriophage M13 genomic DNA (Figures 2A,B and S1). Two other overlap extension PCRs were used to introduce the 5'-stem loop, T7 promoter, ribosome binding site (Table S3) and 3'-spacer region that connected with the scFv library for RD (Figure 2C,D). The RD fragment was approximately 1100-1300 bp (Figure 2D), approximately 5 μg purified PCR product was obtained, and the library contained a capacity of approximately  $5 \times 10^{12}$ . Taken together, the scFv library and RD screening library for breast cancer in various clinical types of stages were successfully established.

## 3.2 | Stem-like cells were enriched and the membrane affinity platform ensured the effectiveness of screening

Fresh breast cancer xenograft tissue was obtained and digested into single cells for primary and suspension culture. After approximately 2 weeks, the shape of the cells presented obvious microsphere growth and the cells could be passaged in vitro (Figure 3A). These microspheres could further differentiate when 1% serum-containing medium was added (Figure 3A). In addition, the microspheres showed a strong ability of collective activities with the movement of irregularly sized microspheres (Figure 3A). Marker detection showed that the proportion of CD44<sup>+</sup> CD24<sup>-</sup> expressing cells was high in

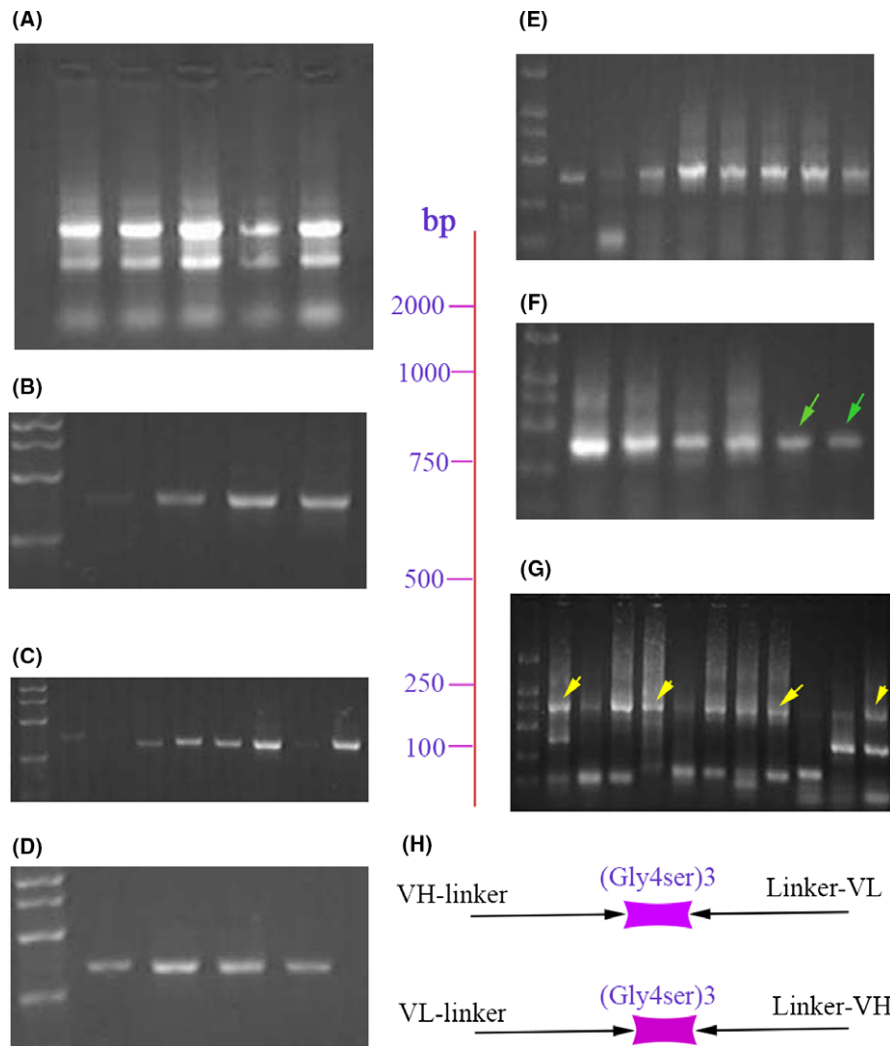


**FIGURE 1** Anti-breast cancer single-chain variable fragment (scFv) library was constructed. A, Total RNA electrophoresis after whole blood lymphocyte separation. B, PCR amplification of VH (approximately 340 bp). C, PCR amplification of the Vk fragment (approximately 325 bp). D, PCR amplification of the Vλ fragment (approximately 325 bp). E, VH-linker amplification with (Gly4Ser)3 (approximately 340-400 bp). F, Linker-VL amplification with (Gly4Ser)3 (approximately 325-400 bp). Linker-Vk and the green arrows indicate the Linker-Vλ. G, Diverse scFv amplification was carried out by splicing by overlap extension PCR followed by electrophoresis (approximately 750 bp). H, Sketch map of diverse scFv libraries

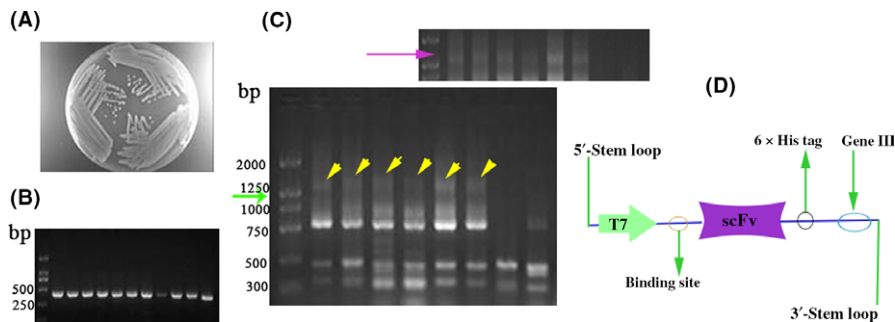


**FIGURE 2** Ribosome display library was constructed. A, Ecoli2738 monoclonal coated plates. B, Electrophoresis of gene III amplification from VCSM13 phage (approximately 330 bp). C, Diverse ribosome display libraries' amplification was carried out by splicing by overlap extension PCR before the electrophoresis (approximately 1100-1300 bp). The green arrow indicates DNA marker and the purple arrow and yellow arrowheads indicate the libraries' fragments. D, Sketch map of the diverse ribosome display library. scFv, single-chain variable fragment

parental MDA-MB-231 cells (Figure 3B). However, in the microspheres, there was a considerably more dynamic balance because they had much higher percentages of CD44<sup>+</sup> CD24<sup>+</sup> and CD44<sup>-</sup> CD24<sup>-</sup> expressing cells. Compared with parental MDA-MB-231, the stemness genes of CD44, SOX2, and OCT4 (Table S4) were all significantly prognostic in the microspheres (Figure 3C).

Next, the active surfaces of these stem-like cell membranes were projected onto the fixed platform, and they showed various forms, such as sheets, spheres, and single cell shapes (Figure 3D). After screening, the cells shrank while the surface of the cell membranes preserved their morphological integrity in general (Figure 3E). Following multiple high-affinity screening, these cell clusters revealed a clear collective inhibition state (Figure 3E). All of these results indicate that the affinity screening platform contained collective microsphere cells with their differentiated and following cells. The screened cell membranes are intact and effective, showing a high affinity; thus, multiple screenings can lead to microspheres' collective inhibition.

### 3.3 | High-affinity scFvs were selected and translation proteins with antitumor features were identified

The mRNAs of scFvs were isolated successfully from the ribosomal complexes. Next, the purified mRNA was reversed to cDNA, and the cDNA was recovered with the identification primers for the new scFv library (Figure 4A). This new scFv library could be amplified with the non-corresponding primers and corresponding primers (Table S3).

Next, the new screening RD fragments were reintroduced with the 5'-stem loop, T7 promoter, ribosome binding site, and 3'-spacer region (Figure 4B, Table S3). After at least three rounds of screening, we obtained a relatively stable scFv library (Figure 4C, scFv 3). Using sequencing and blasting in NCBI BLASTX, the 5'-end contained the specific hits of IGv, and the 3'-end was in line with the non-specific hits of IG-L-κ (Figure S2). By in vitro translation, the results showed that the scFv proteins were expressed from the ribosome complex, as shown by the fluorescent SDS-PAGE staining on the gel (Figure 4D). However, the signals showed that the target ribosome complex proteins were expressed weakly in the first screening, which was located between 25 and 35 kDa (Figure 4D,E). Interestingly, certain high-molecular-weight proteins were also translated (Figure 4E). With multiple selections, the expression of the target scFv proteins were clearly enhanced (Figure 4F). The translation proteins had antitumor activities, as they were in similar positions to the serum-isolated proteins from the breast cancer patients (Figure 4D-F). Taken together, all of the above results indicate that through the repeated cyclic affinity screening, carrying the active and high-affinity of anti-breast cancer, scFvs obtained molecular evolution in vitro.

### 3.4 | Single-chain variable fragments had high affinity with microspheres to inhibit their proliferation

To further clarify the properties of these scFv libraries, we synthesized and validated their effects on microspheres in vitro. After the

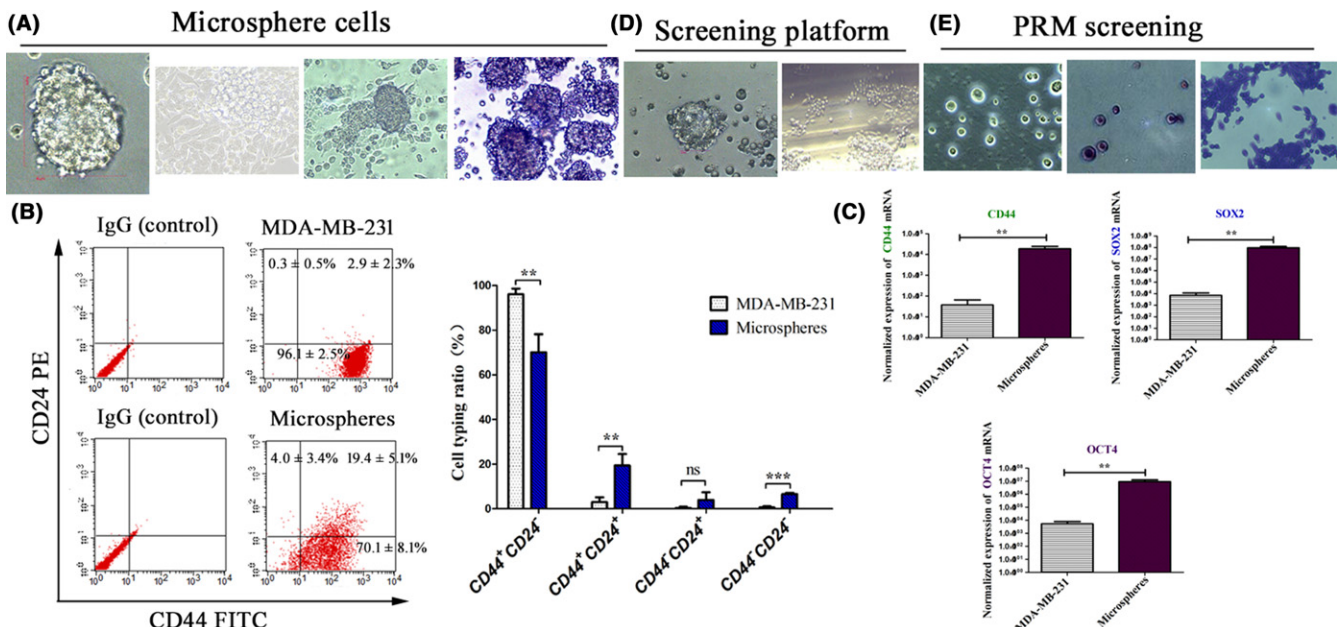


**FIGURE 3** Screening platform of the cell membrane phase was built and applied. A, Microsphere cells were observed by light microscopy: shape at 2 weeks ( $\times 400$ ); differentiation ( $\times 400$ ); collective activity ( $\times 200$ ); and crystal violet solution staining ( $\times 200$ ) shown in panels left to right, respectively. B, Expression profiles of CD44 and CD24 in MDA-MB-231 cells and microspheres. Data are expressed as mean  $\pm$  SD and compared by Student's *t*-test. PE, phycoerythrin. C, Stemness genes were tested by real-time PCR. Normalized gene expression was compared to normal breast cells for standardization. Data are expressed as the mean  $\pm$  SD and compared by Student's *t*-test. D, Screening platform of living fixed stem-like microspheres and differentiated cells ( $\times 200$ ). E, After peptide-ribosome-mRNA (PRM) screening, the fixed stem-like cells and membranes ( $\times 400$ ) and crystal violet staining ( $\times 200$ ); the collective activity of microspheres was inhibited after multiple screening and staining by crystal violet solution ( $\times 200$ ). \**P* < .05; \*\**P* < .01; \*\*\**P* < .001

selected scFvs were added (Figure S2, scFv 3), the proliferation rate of MDA-MB-231 and its microspheres were significantly inhibited, especially over 24 hours and at 100 nmol/L concentration (Figure 5A). This inhibitory effect was clearly enhanced if  $\geq 4$   $\mu\text{g/mL}$  epirubicin was added (Figure 5A). Interestingly, this inhibitory effect was weak for HBL-100 (Figure 5A), and it did not show significant inhibition and toxicity to 293T and HL-7702 cells (Figure S3A). Furthermore, in morphology, the formation, growth, and collective structure of the microspheres were all significantly inhibited (Figure 5B). Through apoptosis detection, the results showed that both the HBL-100 and microspheres did not show a significant apoptosis rate in response to the scFvs. In contrast, the combination therapy significantly increased the microspheres' apoptosis rate, although it was a low concentration of chemotherapeutic agents (Figure 5C).

To test whether the effects on proliferation and apoptosis were related to the antigen and antibody affinity, three 100 nmol/L single scFv incubated for 12 hours were detected with CD44, ALDH1, and CA-153 antigens by ELISA. The data showed that the last selection and synthesis of scFv 3 showed high affinity to all three antigens

(Figure 5D). Furthermore, the luminescence of CD44 and CD24 was clearly decreased and weakened by immunofluorescence when 100 nmol/L scFv was added to the microspheres and incubated for 12 hours (Figure 5E). This influence was not significantly observed in the HBL-100 group (Figure S3B). At the same time, Western blot analysis showed that the expression of CD44 and CD24 was significantly decreased (Figure 5F). All of these results indicate that the scFvs have high affinity with microspheres to inhibit their proliferation, and they have no significant toxicity to HBL-100, 293T, or HL-7702 cells. When combined with chemotherapy, their apoptosis effect on microspheres can be notably enhanced.

### 3.5 | Combination of scFvs and chemotherapy inhibited microsphere invasion and progression

Non-trypsinized treated microspheres and their following intervention groups were tested on Transwell assays (Figure 6A). Quantitative analysis indicated that the numbers of migrating and invading cells in each intervention group were all significantly decreased relative to the microspheres control group (Figure 6A).

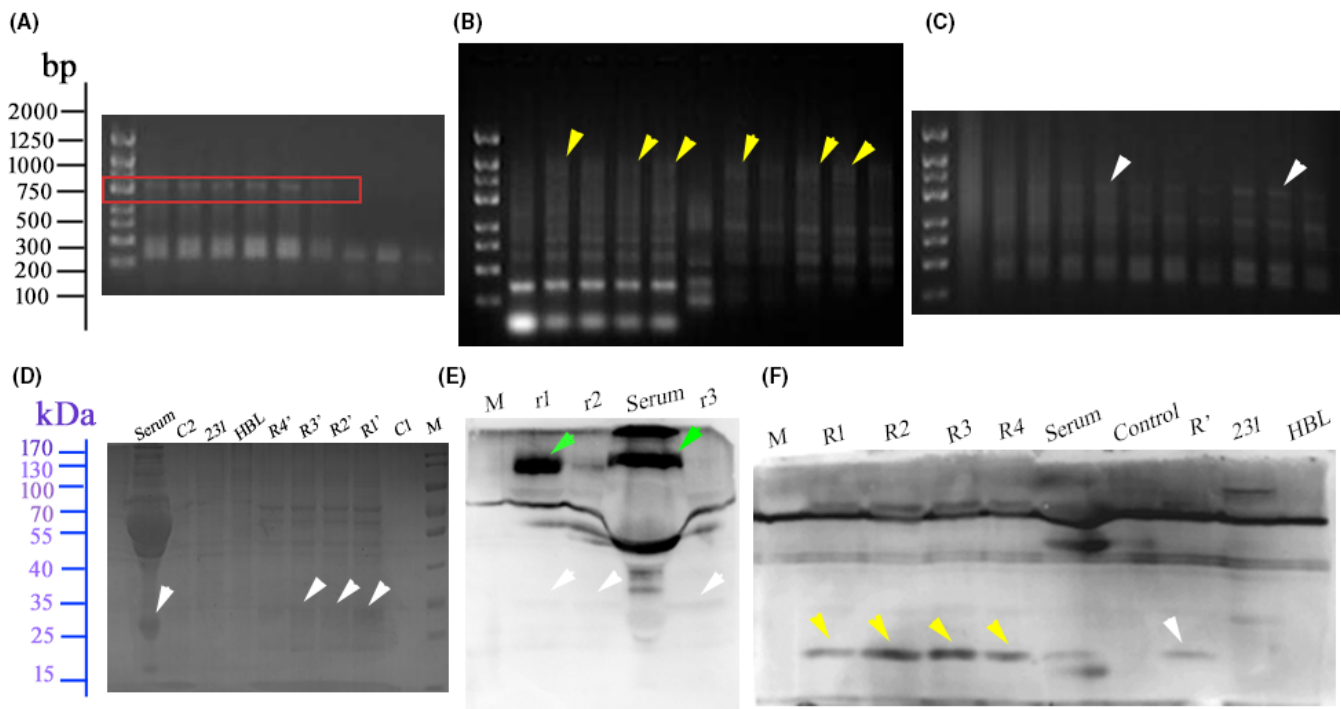


**FIGURE 4** Single-chain variable fragments (scFv) and antitumor proteins acquired from in vitro transcription and translation. A, The peptide-ribosome-mRNA complex was used for in vitro transcription and translation, the first affinity screening of scFv molecules before electrophoresis. B, The new scFv library was reintroduced by the next PCR and new ribosome display library amplification was carried out before electrophoresis. The yellow arrowheads indicate the new ribosome display libraries' fragments. C, Another new scFvs library obtained by multiple elimination and affinity screening. D, Proteins expressed after in vitro translation and shown by fluorescent SDS-PAGE staining on the gel; the target protein size was approximately 25–35 kDa. E, Composite protein expression from the first round of screening. The serum protein came from a screened breast cancer patient. Green arrows indicate high-molecular-weight proteins; white arrows indicate the target proteins. F, Comparative analysis of protein expression after multiple screening. The yellow arrowheads indicate the target proteins after multiple screening. Lane 1, protein marker (M); lanes 2–5, post-translational ribosome complex protein (R1–4); lane 6, serum protein; lane 7, negative control; lane 8, first translation of the ribosomal complex protein (R'); lane 9, MDA-MB-231 protein (231); lane 10, HBL-100 protein (HBL)

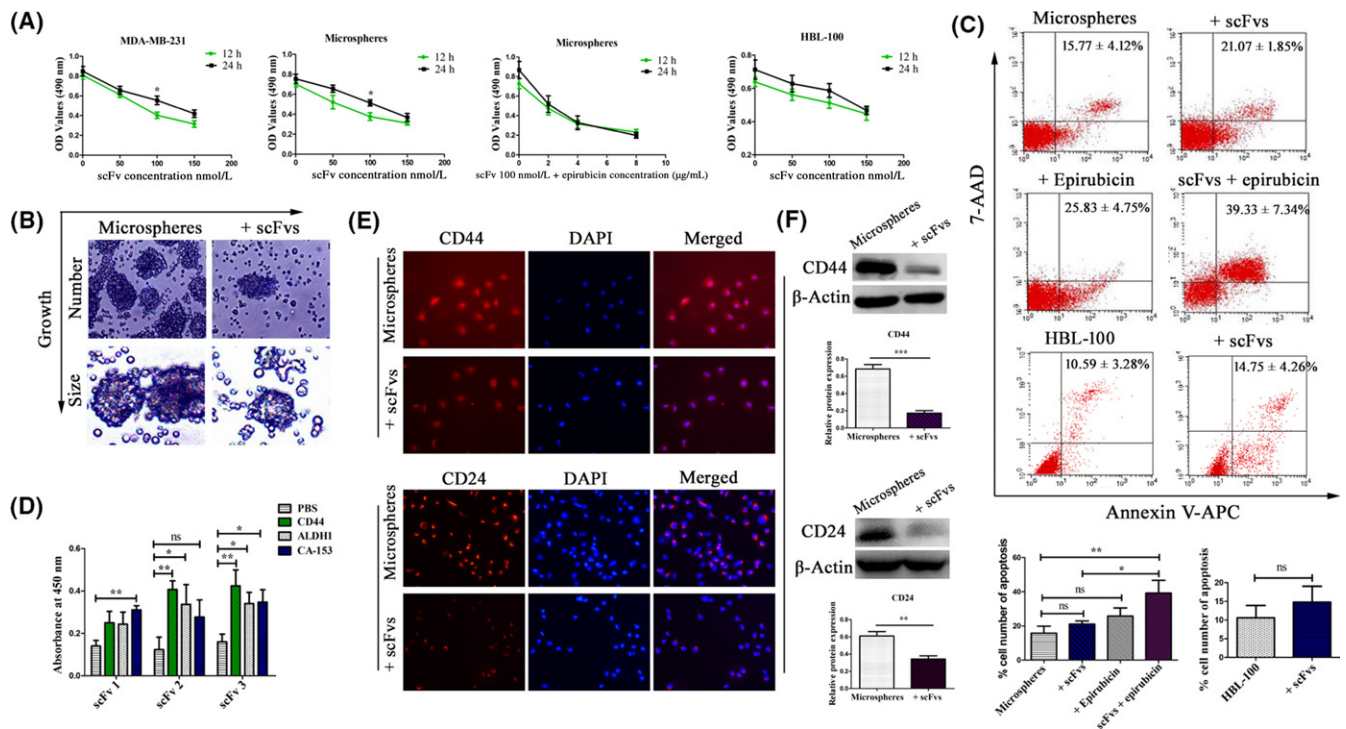


**FIGURE 5** Single-chain variable fragments (scFv) inhibited proliferation of microspheres and showed high affinity to multiple targets. A, MTT assays of cell proliferation showing the effect in each group of cells. Data are expressed as the mean  $\pm$  SEM and the shown comparison in each group was 12-24 hours by *t*-test. B, Growth inhibition of microspheres by 100 nmol/L scFv for 24 hours, staining by crystal violet solution ( $\times 100$ ;  $\times 200$ ). C, Flow cytometry test for the apoptotic changes of each group with 100 nmol/L scFv or 4  $\mu$ g/mL epirubicin. Data are expressed as the mean  $\pm$  SD and compared by *t*-test and one-way ANOVA. 7-AAD, 7-aminoactinomycin D; APC, allophycocyanin. D, ELISA affinity identification of scFv1-3 with CD44, ALDH1, and CA-153. Data are expressed as the mean  $\pm$  SD and compared by one-way ANOVA. E, Immunofluorescence analysis of the CD44 and CD24 markers of cells treated with 100 nmol/L scFv for 12 hours ( $\times 200$ ). (F) Western blot analysis of CD44 and CD24. Data are expressed as the mean  $\pm$  SEM and compared by *t*-test. \**P* < .05; \*\**P* < .01; \*\*\**P* < .001

Interestingly, the scFvs inhibited the microspheres' collective structures and behaviors (Figure 6A). In the *in vivo* study, after the adjacent tumor was subjected to the combination treatment, the growth and volume of tumors were significantly inhibited, and the cumulative treatment could achieve a long stable disease effect (Figure 6B). Liver metastasis (1/5) was only observed in the PBS control group (Figure 6C). There was no significant change in liver, heart, lung, or spleen morphologies in the control and combination treatment groups (Figure 6C). In particular, there was no obvious toxic reaction by the liver, lung, or spleen in the two groups (Figure 6D). The results of immunohistochemistry showed that the expression of PCNA, MMP9, and CD44 were all significantly inhibited in the combination treatment group (Figure 6E).

By further Western blot analysis, both CD44 and CD24 were observed to be expressed at significantly lower levels after the combination treatment (Figure 6F). As we observed that the *ERK*, *p38*, and *JNK* genes are all located in the convergence point of the MAPK pathway, which is closely related to the proliferation and differentiation of stem-like cells (Figure S4), we further detected the expression of these three proteins. The results showed that the proteins were all significantly decreased after the combination treatment (Figure 6G). Taken together, these findings indicate that the proteins related with stemness, growth, and differentiation pathways can be significantly inhibited *in vivo* by

combination treatment. All of these results indicate that scFvs combined with chemotherapy can effectively inhibit tumor metastasis and progression.

## 4 | DISCUSSION

Previous researchers have reported that cancer stem-like microsphere cells can be enriched from their parental cells,<sup>26,27</sup> and microspheres contain a higher proportion of stem cells to proliferate and invade in some collective ways.<sup>4,28</sup> Most interestingly, it has been observed that CSCs or cell clusters leave traces in the circulatory system during their process of metastasis.<sup>6,28</sup> We infer that these traces of metastasis might be identified and remembered by the early antibody immune response. However, these antibody levels are extremely low, far less than direct tumor immune antibody stimulation, nor do they effectively stimulate an immune treatment response. However, these antibodies can be enriched and modified as antitumor antibody libraries, such as the development of CSC-targeted chimeric antigen receptor T cells.<sup>29</sup> In this study, we developed scFv libraries that were sourced from breast cancer patients' peripheral blood lymphocytes and increased the storage capacity of these libraries through mutation and recombination by splicing by overlap extension PCR technology.<sup>30</sup> These libraries included the

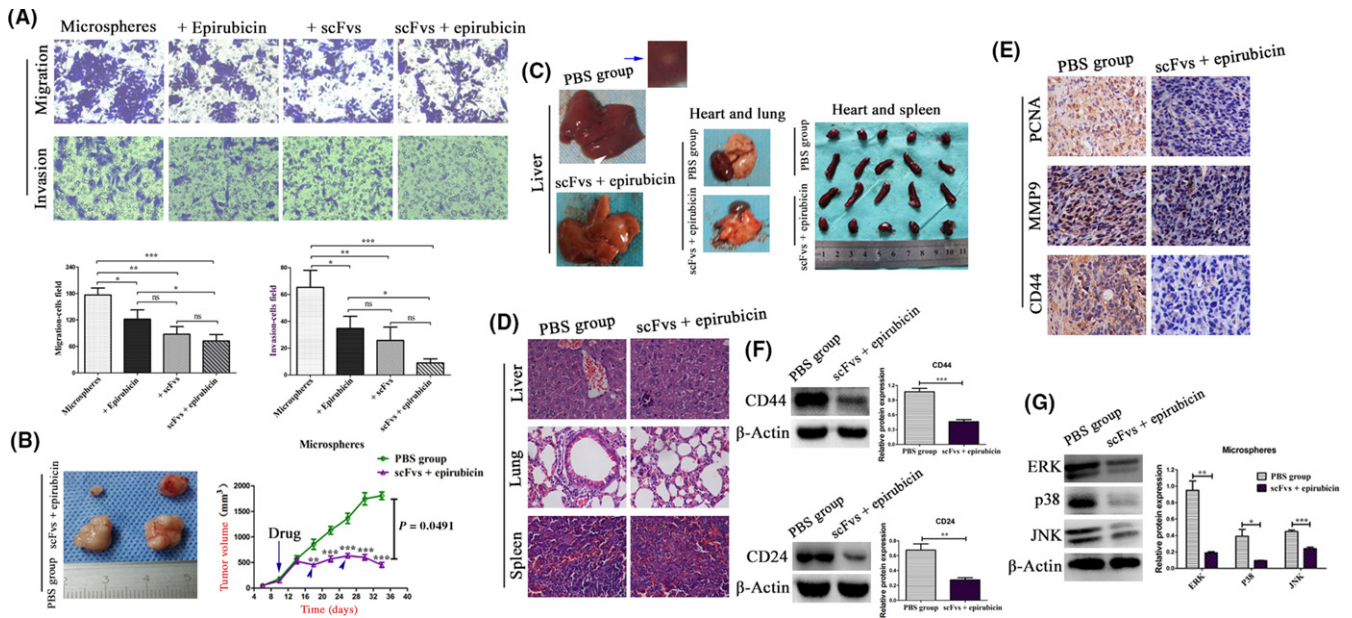


**FIGURE 6** Single-chain variable fragments (scFv) and combination treatment inhibited tumor invasion and progression. A, Microspheres control group and treatment group cells were treated for 24 hours in the upper chamber of 24-well Transwell plates, and the collective migrating and invading cells were representatively imaged ( $\times 200$ ) and quantitatively analyzed. Data are expressed as the mean  $\pm$  SD and compared by one-way ANOVA. B, Analysis of tumor volume and a growth curve of five mice in each group injected with microspheres. The treatment group was injected with the adjacent tumor followed with 100 nmol/L scFv and 4  $\mu$ g/mL epirubicin (30  $\mu$ L) at approximately 10 days. The control group was injected with 60  $\mu$ L PBS. C, Morphologies of liver, heart, lung, and spleen in the two groups. Liver metastasis was only present in the PBS control group (white and blue arrows). D, Morphologies and toxic reaction of the liver, lung, and spleen in both groups by H&E staining ( $\times 200$ ). E, Representative photographs of immunohistochemistry analysis using anti-PCNA, anti-MMP9, and anti-CD44 staining in both groups ( $\times 200$ ). F, Western blot analysis of CD44 and CD24 in the two groups. G, Western blot analysis of ERK, p38, and JNK. Data are expressed as the mean  $\pm$  SEM and compared by *t*-test. \* $P < .05$ ; \*\* $P < .01$ ; \*\*\* $P < .001$

natural immune information, which might reflect the current disease state of the patients (Table S1). For instance, we found a higher Leu/Lym rate from cancer patients could build more stable libraries (Table S1).<sup>31,32</sup> Our results suggested that there was a positive relationship between the degree of immunity and the antibody library. Our data showed that the construction of scFv libraries from peripheral blood in early stage cancer was also reliable, and it might not be related to the stage and type of tumors.

Screening antibody molecules that take into account stem-like cells and cancer cells should be one of the directions for future research on immunity.<sup>20,26</sup> Thus, our screening methods were not only based on the affinity to the microspheres but also dependent on the selective effect on their early differentiated cells.<sup>4,19,28</sup> This approach ensured that subsequent identification and treatment was effective both for the microspheres and cancer cells (Figure 3). The solid platform display technology has been shown to be mature *in vitro*.<sup>33,34</sup> In this study, we used the microspheres as a screening platform, which kept the cell membrane surface antigens complete and similar to their natural characteristics. Through the direct screening of antibodies without prior experience in intact cells, some unknown and affinity ligands were found (Figure 4D-F). This showed that we obtained high-affinity scFvs that combined with microspheres by repeated panning, which showed high affinity to CD44 and CD24 (Figure 5E, F). Our results showed that the scFvs changed *in vitro* to identify

a variety of different antigens (Figure 5D,E), following Darwin's evolutionary theory.<sup>11,14,35</sup>

Ribosome display technology can select even nanomolar concentrations of a DNA template library.<sup>10</sup> Through the amplification of PCR, the trace mRNA can be released and detected from the mRNA-peptide affinity of the ribosome complex. These new mRNAs can be used for the next round of screening, and they can also be amplified, sequenced, and cloned into vectors.<sup>35,36</sup> In this study, we showed the screening molecular banding and we repeatedly purified, sequenced, and amplified the target products (Figure S2). Previous research has shown that PCR is also a convenient mutagenesis strategy<sup>37</sup>; therefore, the results of iterations between diversification and selection allow for protein evolution *in vitro* by RD.<sup>36,38</sup> We showed that proteins were expressed from the ribosome complex in *in vitro* translation (Figure 4D-F). At the beginning, the target band was weak, but several high-molecular-weight proteins were expressed (Figure 4E). The target proteins could be enhanced and enriched in multiple rounds of screening. We showed that the translated proteins had some antitumor activity because they were located in a similar position to the serum protein that was isolated from the breast cancer patient, whereas both the breast cancer and HBL-100 cells lacked the biotinylated proteins (Figure 4D-F). Therefore, the successful implementation of RD allowed us to obtain the evolved scFvs, which can synthesize high-affinity proteins against targets (Figures 4 and S2d).

Chimeric antigen receptor T cell technology is an important technology with rapid development in recent years.<sup>39,40</sup> However, its application in the treatment of solid tumors is relatively limited, and the function of scFvs has not been completely discussed.<sup>41</sup> In this study, we showed that selected scFvs significantly inhibited the proliferation and invasion of microspheres at a certain concentration (Figure 5A). Interestingly, the high-affinity targets might be CD44<sup>+</sup>/CD24<sup>+</sup>. As CD44<sup>+</sup> CD24<sup>-</sup> and CD44<sup>+</sup> CD24<sup>+</sup> were both highly expressed in the microspheres and MDA-MB-231 cells (Figure 3A), we believed that our selected scFvs could inhibit the related effects of stemness, proliferation, and differentiation at the same time, which could cause a chain reaction.<sup>42,43</sup> It was shown that the combination treatment significantly reduced the MAPK pathway proteins' expression, and we considered the MAPK pathway to be another shared pathway of CSCs and cancer cells (Figures 6G and S3). No significant toxic reaction of the scFvs has been observed on normal cells and tissues in either single or combination treatments (Figures 6C,D and S3). Except for the high-affinity effect, this might partly be reflected to disperse the spherical structure of microspheres and inhibit their collective behaviors, while showing no obvious effect on apoptosis (Figures 5B,C and 6A). However, the apoptosis effect of microspheres was significantly promoted when the combination treatment was used. In another way, this synergistic effect of molecular combination chemotherapy is similar to the research into aptamers.<sup>25,44,45</sup> Taking scFvs as aptamers, they will be more beneficial to clinical treatment, as they are much more capable of mass synthesis, further editing, and modification (Figure S2). In addition, the scFvs have been considered for wide use against many kinds of tumors.<sup>46</sup> Thus, the screening scFvs might be another effective immune and molecular therapy method, as they have a synergistic effect on clusters of microspheres and cancer cells. We consider that this synergistic effect might be due to high-affinity precise binding and then inhibition of the shared stemness and proliferation signaling pathways in CSCs and cancer cells.

In summary, this study showed that scFvs from dynamic screening by RD in a natural state could result in high-affinity evolution to recognize microspheres. The scFvs could effectively inhibit the collective growth and invasion of microspheres through targets that might be CD44<sup>+</sup>/CD24<sup>+</sup>. When combined with chemotherapy, the scFvs showed enhancement of their high-affinity efficiency in inhibiting the proliferation and invasion of microspheres in vitro and in vivo.

## ACKNOWLEDGMENTS

This work was supported by grants from the National Natural Science Foundation of China (No. 81272898). We sincerely thank Professor Wei Duan (Deakin University, Australia) for fruitful discussions.

## CONFLICT OF INTEREST

The authors have no conflict of interest.

## ORCID

Shangke Huang  <http://orcid.org/0000-0002-9356-7588>

## REFERENCES

1. Yoshida GJ, Saya H. Therapeutic strategies targeting cancer stem cells. *Cancer Sci*. 2016;107:5-11.
2. Jordan NV, Bardia A, Wittner BS, et al. HER2 expression identifies dynamic functional states within circulating breast cancer cells. *Nature*. 2016;537:102-106.
3. Weitzenfeld P, Meshel T, Ben-Baruch A. Microenvironmental networks promote tumor heterogeneity and enrich for metastatic cancer stem-like cells in Luminal-A breast tumor cells. *Oncotarget*. 2016;7:81123-81143.
4. Cheung KJ, Padmanaban V, Silvestri V, et al. Polyclonal breast cancer metastases arise from collective dissemination of keratin 14-expressing tumor cell clusters. *Proc Natl Acad Sci USA*. 2016;113:E854-E863.
5. Fidler IJ. The pathogenesis of cancer metastasis: the 'seed and soil' hypothesis revisited. *Nat Rev Cancer*. 2003;3:453-458.
6. Aceto N, Bardia A, Miyamoto DT, et al. Circulating tumor cell clusters are oligoclonal precursors of breast cancer metastasis. *Cell*. 2014;158:1110-1122.
7. Hong IS, Lee HY, Nam JS. Cancer stem cells: the 'Achilles heel' of chemo-resistant tumors. *Recent Pat Anticancer Drug Discov*. 2015;10:2-22.
8. Boral D, Nie D. Cancer stem cells and niche microenvironments. *Front Biosci (Elite Ed)*. 2012;4:2502-2514.
9. Hardin H, Zhang R, Helein H, Buehler D, Guo Z, Lloyd RV. The evolving concept of cancer stem-like cells in thyroid cancer and other solid tumors. *Lab Invest*. 2017;97:1142-1151.
10. Dreier B, Pluckthun A. Rapid selection of high-affinity binders using ribosome display. *Methods Mol Biol*. 2012;805:261-286.
11. Bradbury AR, Sidhu S, Dubel S, McCafferty J. Beyond natural antibodies: the power of in vitro display technologies. *Nat Biotechnol*. 2011;29:245-254.
12. Pansri P, Jaruseranee N, Rangnoi K, Kristensen P, Yamabhai M. A compact phage display human scFv library for selection of antibodies to a wide variety of antigens. *BMC Biotechnol*. 2009;9:6.
13. Schaffitzel C, Hanes J, Jermutus L, Pluckthun A. Ribosome display: an in vitro method for selection and evolution of antibodies from libraries. *J Immunol Methods*. 1999;231:119-135.
14. Beene DL, Dougherty DA, Lester HA. Unnatural amino acid mutagenesis in mapping ion channel function. *Curr Opin Neurobiol*. 2003;13:264-270.
15. Rothe A, Nathanielsz A, Oberhauser F, et al. Ribosome display and selection of human anti-cD22 scFvs derived from an acute lymphocytic leukemia patient. *Biol Chem*. 2008;389:433-439.
16. Mu W, Hu C, Zhang H, et al. miR-27b synergizes with anticancer drugs via p53 activation and CYP1B1 suppression. *Cell Res*. 2015;25:477-495.
17. Li W, Ma H, Zhang J, Zhu L, Wang C, Yang Y. Unraveling the roles of CD44/CD24 and ALDH1 as cancer stem cell markers in tumorigenesis and metastasis. *Sci Rep*. 2017;7:13856.
18. Al-Hajj M, Wicha MS, Benito-Hernandez A, Morrison SJ, Clarke MF. Prospective identification of tumorigenic breast cancer cells. *Proc Natl Acad Sci USA*. 2003;100:3983-3988.
19. Rostoker R, Abelson S, Genkin I, et al. CD24(+) cells fuel rapid tumor growth and display high metastatic capacity. *Breast Cancer Res*. 2015;17:78.
20. Reya T, Morrison SJ, Clarke MF, Weissman IL. Stem cells, cancer, and cancer stem cells. *Nature*. 2001;414:105-111.

21. Lee MH, Yoon DS. A phenotype-based RNAi screening for Ras-ERK/ MAPK signaling-associated stem cell regulators in *C. elegans*. *Methods Mol Biol*. 2017;1622:207-221.
22. Leedham SJ. MAP(K)ing the path to stem cell quiescence and the elusive enteroendocrine cell. *Cell Stem Cell*. 2017;20:153-154.
23. Balko JM, Schwarz LJ, Bhola NE, et al. Activation of MAPK pathways due to DUSP4 loss promotes cancer stem cell-like phenotypes in basal-like breast cancer. *Cancer Res*. 2013;73:6346-6358.
24. Marks JD, Hoogenboom HR, Bonnert TP, McCafferty J, Griffiths AD, Winter G. By-passing immunization. Human antibodies from V-gene libraries displayed on phage. *J Mol Biol*. 1991;222:581-597.
25. Xiang D, Zheng C, Zhou SF, et al. Superior performance of aptamer in tumor penetration over antibody: implication of aptamer-based theranostics in solid tumors. *Theranostics*. 2015;5:1083-1097.
26. Charafe-Jauffret E, Ginestier C, Iovino F, et al. Breast cancer cell lines contain functional cancer stem cells with metastatic capacity and a distinct molecular signature. *Cancer Res*. 2009;69:1302-1313.
27. Ishiguro T, Ohata H, Sato A, Yamawaki K, Enomoto T, Okamoto K. Tumor-derived spheroids: relevance to cancer stem cells and clinical applications. *Cancer Sci*. 2017;108:283-289.
28. Konen J, Summerbell E, Dwivedi B, et al. Image-guided genomics of phenotypically heterogeneous populations reveals vascular signalling during symbiotic collective cancer invasion. *Nat Commun*. 2017;8:15078.
29. Guo Y, Feng K, Wang Y, Han W. Targeting cancer stem cells by using chimeric antigen receptor-modified T cells: a potential and curable approach for cancer treatment. *Protein Cell*. 2017; <https://doi.org/10.1007/s13238-017-0394-6>
30. Gu L, Li C, Aach J, Hill DE, Vidal M, Church GM. Multiplex single-molecule interaction profiling of DNA-barcoded proteins. *Nature*. 2014;515:554-557.
31. Templeton AJ, Knox JJ, Lin X, et al. Change in neutrophil-to-lymphocyte ratio in response to targeted therapy for metastatic renal cell carcinoma as a prognosticator and biomarker of efficacy. *Eur Urol*. 2016;70:358-364.
32. Ocana A, Nieto-Jimenez C, Pandiella A, Templeton AJ. Neutrophils in cancer: prognostic role and therapeutic strategies. *Mol Cancer*. 2017;16:137.
33. Zhao A, Tohidkia MR, Siegel DL, Coukos G, Omid Y. Phage antibody display libraries: a powerful antibody discovery platform for immunotherapy. *Crit Rev Biotechnol*. 2016;36:276-289.
34. Rothe A, Hosse RJ, Power BE. Ribosome display for improved bio-therapeutic molecules. *Expert Opin Biol Ther*. 2006;6:177-187.
35. Ohashi H, Kanamori T, Osada E, Akbar BK, Ueda T. Peptide screening using PURE ribosome display. *Methods Mol Biol*. 2012;805:251-259.
36. Zahnd C, Amstutz P, Pluckthun A. Ribosome display: selecting and evolving proteins in vitro that specifically bind to a target. *Nat Methods*. 2007;4:269-279.
37. Chodorge M, Fourage L, Ravot G, Jermutus L, Minter R. In vitro DNA recombination by L-Shuffling during ribosome display affinity maturation of an anti-Fas antibody increases the population of improved variants. *Protein Eng Des Sel*. 2008;21:343-351.
38. Dreier B, Pluckthun A. Ribosome display: a technology for selecting and evolving proteins from large libraries. *Methods Mol Biol*. 2011;687:283-306.
39. June CH, Maus MV, Plesa G, et al. Engineered T cells for cancer therapy. *Cancer Immunol Immunother*. 2014;63:969-975.
40. Abramson JS, McGree B, Noyes S, et al. Anti-CD19 CAR T cells in CNS diffuse large-B-cell lymphoma. *N Engl J Med*. 2017;377:783-784.
41. Yang Y, Jacoby E, Fry TJ. Challenges and opportunities of allogeneic donor-derived CAR T cells. *Curr Opin Hematol*. 2015;22:509-515.
42. Jaggupilli A, Elkord E. Significance of CD44 and CD24 as cancer stem cell markers: an enduring ambiguity. *Clin Dev Immunol*. 2012;2012:708036.
43. Keysar SB, Jimeno A. More than markers: biological significance of cancer stem cell-defining molecules. *Mol Cancer Ther*. 2010;9:2450-2457.
44. Xiang D, Shigdar S, Qiao G, et al. Nucleic acid aptamer-guided cancer therapeutics and diagnostics: the next generation of cancer medicine. *Theranostics*. 2015;5:23-42.
45. AlShamaileh H, Wang T, Xiang D, et al. Aptamer-mediated survivin RNAi enables 5-fluorouracil to eliminate colorectal cancer stem cells. *Sci Rep*. 2017;7:5898.
46. Inoue Y, Matsuura S, Yoshimura K, et al. Characterization of V-set and immunoglobulin domain containing 1 exerting a tumor suppressor function in gastric, lung, and esophageal cancer cells. *Cancer Sci*. 2017;108:1701-1714.

## SUPPORTING INFORMATION

Additional Supporting Information may be found online in the supporting information tab for this article.

**How to cite this article:** Huang S, Feng L, An G, et al. Ribosome display and selection of single-chain variable fragments effectively inhibit growth and progression of microspheres in vitro and in vivo. *Cancer Sci*. 2018;109:1503-1512. <https://doi.org/10.1111/cas.13574>